



**HAL**  
open science

## Contrasting Arsenic biogeochemical cycling in two Moroccan alkaline pit lakes

Marina Hery, Angelique Desoeuvre, El Mehdi Benyassine, Odile Bruneel, S. Delpoux, Eleonore Resongles, Abdelilah Dekayir, Corinne Casiot

► **To cite this version:**

Marina Hery, Angelique Desoeuvre, El Mehdi Benyassine, Odile Bruneel, S. Delpoux, et al.. Contrasting Arsenic biogeochemical cycling in two Moroccan alkaline pit lakes. *Research in Microbiology*, 2020, 171 (1), pp.28-36. 10.1016/j.resmic.2019.10.007 . hal-02339031

**HAL Id: hal-02339031**

**<https://hal.science/hal-02339031>**

Submitted on 15 May 2020

**HAL** is a multi-disciplinary open access archive for the deposit and dissemination of scientific research documents, whether they are published or not. The documents may come from teaching and research institutions in France or abroad, or from public or private research centers.

L'archive ouverte pluridisciplinaire **HAL**, est destinée au dépôt et à la diffusion de documents scientifiques de niveau recherche, publiés ou non, émanant des établissements d'enseignement et de recherche français ou étrangers, des laboratoires publics ou privés.

# Journal Pre-proof



Contrasting Arsenic biogeochemical cycling in two Moroccan alkaline pit lakes

Marina Héry, Angélique Desoeuvre, El Mehdi Benyassine, Odile Bruneel, Sophie Delpoux, Eléonore Resongles, Abdelilah Dekayir, Corinne Casiot

PII: S0923-2508(19)30125-1

DOI: <https://doi.org/10.1016/j.resmic.2019.10.007>

Reference: RESMIC 3750

To appear in: *Research in Microbiology*

Received Date: 16 April 2019

Revised Date: 23 October 2019

Accepted Date: 23 October 2019

Please cite this article as: M. Héry, A. Desoeuvre, E.M. Benyassine, O. Bruneel, S. Delpoux, E. Resongles, A. Dekayir, C. Casiot, Contrasting Arsenic biogeochemical cycling in two Moroccan alkaline pit lakes, *Research in Microbiology*, <https://doi.org/10.1016/j.resmic.2019.10.007>.

This is a PDF file of an article that has undergone enhancements after acceptance, such as the addition of a cover page and metadata, and formatting for readability, but it is not yet the definitive version of record. This version will undergo additional copyediting, typesetting and review before it is published in its final form, but we are providing this version to give early visibility of the article. Please note that, during the production process, errors may be discovered which could affect the content, and all legal disclaimers that apply to the journal pertain.

© 2019 Published by Elsevier Masson SAS on behalf of Institut Pasteur.

1 Contrasting Arsenic biogeochemical cycling in two Moroccan alkaline pit lakes

2

3 Marina Héry<sup>1\*</sup>, Angélique Desoeuvre<sup>1</sup>, El Mehdi Benyassine<sup>2</sup>, Odile Bruneel<sup>1</sup>, Sophie

4 Delpoux<sup>1</sup>, Eléonore Resongles<sup>1</sup>, Abdelilah Dekayir<sup>2</sup>, Corinne Casiot<sup>1</sup>.

5

6 <sup>1</sup> HydroSciences Montpellier, University of Montpellier, CNRS, IRD, Montpellier, France.

7 <sup>2</sup> Equipe Géoexplorations & Géotechniques, University Moulay Ismail, BP.11201, Zitoune,

8 Meknes, Morocco.

9

10 [marina.hery@umontpellier.fr](mailto:marina.hery@umontpellier.fr) \*Correspondence and reprints

11 [angelique.desoeuvre@umontpellier.fr](mailto:angelique.desoeuvre@umontpellier.fr)

12 [benyassine.elmehdi@gmail.com](mailto:benyassine.elmehdi@gmail.com)

13 [odile.bruneel@ird.fr](mailto:odile.bruneel@ird.fr)

14 [eleonore.resongles@umontpellier.fr](mailto:eleonore.resongles@umontpellier.fr)

15 [sophie.delpoux@umontpellier.fr](mailto:sophie.delpoux@umontpellier.fr)

16 [dekayir@yahoo.fr](mailto:dekayir@yahoo.fr)

17 [corinne.casiot-marouani@umontpellier.fr](mailto:corinne.casiot-marouani@umontpellier.fr)

18

19

## 20 Abstract

21 Pit lakes resulting from the flooding of abandoned mines represent a valuable freshwater  
22 reserve. However, water contamination by toxic elements, including arsenic, compromises  
23 their use for freshwater supply. For a better management of these reserves, our aim was to  
24 gain insight into arsenic cycling in two Moroccan alkaline pit lakes. We first showed that  
25 dimethylarsenic dominated in stratified lake ZA whereas in lake ZL1, As(V) was prevailing.  
26 Because microbially mediated processes largely contribute to arsenic cycling, the diversity of  
27 arsenic-methylating and -oxidizing bacteria was determined through the sequencing of *arsM*  
28 and *aioA* genes. Diverse *arsM*-carrying bacteria were thriving in ZA while a low diversity of  
29 *aioA* genes was detected in ZL1. We also determined the structure of the total bacterial  
30 communities by fingerprinting (ARISA). Contrasting arsenic speciation and bacterial  
31 communities in the two lakes were associated with differences of conductivity, Total Organic  
32 Carbon and temperature. In ZA, dissolved oxygen and redox potential were the main factors  
33 driving the total bacterial community structure and the *ArsM* diversity. In ZL1, stable  
34 bacterial communities were associated with limited water physico-chemistry variations. Our  
35 study provides new insights into the biogeochemical behavior of arsenic and the role of  
36 arsenic transforming bacteria in alkaline pit lakes.

37

38 **Keywords:** arsenic; biotransformation; alkaline pit lake; methylation; oxidation.

## 39 1. Introduction

40 Mining of metalliferous deposits leads to excavation of large amounts of rocks  
41 resulting in open pits where mineralized rocks are exposed to weathering. As rainwater  
42 accumulates and groundwater rebounds, a lake may form inside the mine pit. Lake waters

43 represent precious freshwater supply, especially in areas suffering from deficient water  
44 resources as in semi-arid area in southern Mediterranean countries. However, the potential  
45 release of metals and metalloids from mineralized rocks seriously jeopardizes the safe use of  
46 this freshwater resource. Among these toxic elements, arsenic represents a threat for  
47 environmental and public health. Arsenic is widespread in mining areas where it is frequently  
48 associated with the exploited metal sulfides [1].

49 In Morocco, opencast mining operations of metal sulfides left a number of pit lakes  
50 which are currently used for irrigation and livestock watering [2-4]. These lakes exhibit near-  
51 neutral to alkaline pH due to the predominance of carbonate rocks [5]. Arsenic concentrations  
52 exceeding Moroccan standards for irrigation water have been measured in these lakes [2-4].  
53 The release of arsenic from mine pit wall is favored at alkaline pH because arsenic oxyanions,  
54 arsenite ( $\text{H}_2\text{AsO}_3^-$ ) and arsenate ( $\text{HAsO}_4^{2-}$ ), hardly sorb to the surfaces of negatively charged  
55 iron oxyhydroxides [6,7].

56 Microorganisms have evolved diverse strategies to transform arsenic for detoxification  
57 or metabolism purpose) [8,9]. Arsenic microbially mediated biotransformations are highly  
58 relevant to the global arsenic cycling in the environment [10]. Many bacteria have the ability  
59 to oxidize arsenite into less toxic and less mobile arsenate [11-14], for detoxification purposes  
60 or energy generation. This function is conferred by an arsenite oxidase (encoded by *aio* gene)  
61 [15-17]. Another type of As(III) oxidase was identified in 2010 in haloalkaliphile  
62 *Alkalilimnicola ehrlichii* MLHE-1. In this strain isolated from Mono Lake, the oxidation of  
63 arsenite is coupled to the reduction of nitrate and carried out by a new gene family called *arxA*  
64 [18]. Some microorganisms have the capacity to transform arsenite into methylated forms  
65 [19]. This biomethylation process involves the S-adenosylmethionine methyltransferase  
66 encoded by *arsM* genes [20]. Methylated As species, both volatile (e.g. trimethylarsenic  
67 (TMA) and trimethylarsine (TMAO) and non-volatile (e.g. monomethylarsenic (MMA) and

68 dimethylarsenic (DMA)), are less toxic than their inorganic forms [21]. Thus, biomethylation  
69 is generally considered as one of the main detoxification pathways for As in the environment  
70 [22]. However, because some intermediate products are highly toxic, arsenic biomethylation  
71 as a detoxification process has been questioned [21, 23-24]. Finally, under reducing  
72 conditions, dissimilatory arsenate-reducing prokaryotes use As(V) as final electron acceptor  
73 for anaerobic respiration [25].

74         So far, attention has been mainly focused on arsenic biogeochemistry in paddy soils  
75 [26], marine waters [27-28], groundwater used as drinking water (for a recent review see  
76 [29]), or in extreme environments such as soda lakes located in geothermal regions [30-31]. In  
77 comparison, the question of the microbially mediated transformations of arsenic in alkaline  
78 mine pit lakes, characterized by a moderate salinity (conductivity) compared to soda lakes  
79 ( $6.1-15.5 \text{ mS/cm}^{-1}$  in ZA or ZL1 compared to  $42-86 \text{ mS/cm}^{-1}$  in Mono Lake,) has received  
80 little attention. Such alkaline pit lakes are common along the southern margin of the  
81 Mediterranean Sea, where metal deposits occur within carbonated layers of Mesozoic and  
82 Tertiary sediments [5,32].

83         In the present study, we investigated the spatial and seasonal dynamics of arsenic  
84 concentrations (total dissolved As and its species arsenite, arsenate, monomethylarsenic  
85 (MMA) and dimethylarsenic (DMA)) in two Moroccan alkaline pit lakes used for irrigation  
86 and livestock watering. The dynamic of the whole bacterial community thriving in these lakes  
87 was assessed by an automated fingerprinting approach (Automated Ribosomal Intergenic  
88 Spacer Analysis [33]). ARISA has a similar capacity as metabarcoding to discriminate  
89 environmental samples and to correlate bacterial community structure with environmental  
90 variables [34]. To gain insight into the biogeochemical processes controlling arsenic  
91 speciation in these environments, and based on arsenic speciation results, we specifically

92 targeted microbial populations involved in arsenic oxidation and biomethylation through the  
93 study of their respective marker genes *aioA* and *arsM*.

94

## 95 **2. Materials and methods**

### 96 *2.1. Site description*

97 The Zeida mining area is located in the High Moulouya basin. It is bounded by the High Atlas  
98 on the southeast and by the Middle Atlas on the northwest (Fig. 1A). The geology of the area  
99 has been described in [4] and [35]. The climatic conditions in the upper Moulouya region are  
100 semi-arid, with annual precipitation of 100–400 mm and mean annual temperatures of 12–  
101 14°C. The region faces a rainfall deficit caused by recurrent droughts. Lead has been  
102 exploited until 1985, from lead–barite ores [2]. In Zeida, the exploited orebody consisted  
103 mainly of cerussite [ $\text{PbCO}_3$ ] (70%) and galena [ $\text{PbS}$ ] (30%) [36]. After mining activity  
104 ceased, the region shifted into livestock breeding and orchards (apple trees).

105 The two pit lakes under study were lake ZA (32°50.112' N, 04°57.223' W), with a  
106 volume of 1  $\text{Mm}^3$ , and lake ZL1 (32°47.517' N, 04°58.815' W), with a volume of 2  $\text{Mm}^3$ .  
107 They are located respectively 2 km north-east and 5 km south-west from the small town of  
108 Zeida (Fig. 1A). ZA is located next to the waste pile of the ore treatment facility of Zeida  
109 which treated the ore by mechanical (crushing at 250 mm, grinding at 0.3 mm) and chemical  
110 processes (flotation with the use of sulfhydrate sodium amyloxanthate, sodium silicate and pine  
111 tree oil) (Fig. 1B). ZL1 is surrounded by tailings material from ore excavation (Fig. 1C).

112

### 113 *2.2. Sampling*

114 In October 2012 and in July 2013, water samples (1 L) were collected from a boat in lake  
115 ZA and lake ZL1, at the surface and the bottom of the lakes (5 m depth for lake ZA, 12.5 m  
116 depth for lake ZL1), using a Merkos sampler (Hydro-bios, Germany). The main physico-

117 chemical parameters (pH, temperature, redox potential, conductivity and dissolved oxygen  
118 concentration) were measured *in situ* as soon as the sampler was taken out of the water using  
119 an HQ40d portable multi-parameter (HACH Co., Loveland, CO, USA) equipped with a  
120 refillable standard pH liquid electrode (pHC30101), a standard conductivity electrode  
121 (CDC40101), a gel filled ORP electrode (MTC10101) and a standard LDO electrode  
122 (LDO10101).

### 123 2.3. Sample treatment and chemical analyses

124 Fifty milliliters of unfiltered water was used for the analysis of bicarbonate and  
125 carbonate by titration with standardized HCl 0,1 N. For total organic carbon, samples (60 ml)  
126 were taken in amber glass bottles previously decontaminated by heating at 550 °C, preserved  
127 by adding H<sub>3</sub>PO<sub>4</sub> 1:1000 (v:v) and analyzed within 2 weeks. Another 200 ml of water were  
128 filtered in the field through 0.22 µm Millipore membranes fitted on Sartorius polycarbonate  
129 filter holders. Subsamples were preserved for the analysis of major anions (Cl<sup>-</sup>, SO<sub>4</sub><sup>2-</sup>) and  
130 cations (Na<sup>+</sup>, K<sup>+</sup>, Mg<sup>2+</sup>, Ca<sup>2+</sup>), trace elements and arsenic speciation according to the routine  
131 procedures described in [37] and analyzed within a few days after collection.

132 Inorganic and methylated arsenic species (As(III), As(V), MMA and DMA) were  
133 analyzed using anion-exchange chromatography (25 cm × 4.1 mm i.d. Hamilton PRP-X100  
134 column and SpectraSystem P4000 ThermoScientific pump) coupled to ICP-MS (Thermo X7  
135 Series), in gradient elution mode, with an ammonium phosphate eluent, as described in [38].  
136 Analysis of major cations and anions was carried out using ion chromatography (Dionex ICS-  
137 1000). Total organic carbon concentration was determined using a high-temperature catalytic  
138 oxidation method (HTCO), with a Shimadzu TOC-VCSH total organic carbon analyzer.  
139 Analysis of trace elements (Mn, Al, Zn, Pb, and Fe) was carried out using ICP-MS (Thermo  
140 X7 Series), as described elsewhere [37].

141 To estimate the photosynthetic microbial biomass, Chlorophyll a (Chla) was  
142 quantified on 300 ml samples of lake waters previously filtrated on glass fiber filters  
143 according to the method NF T 90 -117 (Centre d'analyses Méditerranée Pyrénées,  
144 Perpignan, France).

145

#### 146 *2.4 Sample treatment and microbial analysis*

147 Microbial analyses were performed on water samples from the surface and the bottom  
148 of each lake, for the two sampling campaigns. For each water sample, six aliquots of 250 ml  
149 were filtrated in the field through 0.22 µm cellulose acetate filter (Sartorius stedim biotech,  
150 Aubagne, France) to obtain six replicates. Each filter was immediately transferred to a  
151 cryotube, kept at 4°C in a container with ice packs before reaching the laboratory and frozen  
152 at -80°C until DNA extraction. This protocol was applied in October 2012 for ZL1 lake and in  
153 July 2013 for ZA and ZL1 lakes. For ZA lake in October 2012, an alternative treatment was  
154 used to collect the microbial biomass; indeed, the high suspended matter content prevented  
155 the filtration of ZA lake waters *in situ*. Water samples (300 ml, in triplicate) were centrifuged  
156 (6,000 g, 20 min) back to the laboratory to pellet the microbial cells. The cell pellets were  
157 stored at -20°C until DNA extraction. Samples were named as follow: ZAsO12 for ZA lake  
158 sampled at the surface in October 2012, ZAbO12 for ZA lake sampled at the bottom in  
159 October 2012, ZAsJ13 and ZAbJ13 for ZA in July 2013, ZL1sO12 and ZL1bO12 for ZL1 in  
160 October 2012, ZL1sJ13 and ZL1bJ13 for ZL1 in July 2013.

161

##### 162 *2.4.1. Microbial DNA isolation and Automated Ribosomal Intergenic Spacer Analysis* 163 *(ARISA)*

164 Total DNA was extracted from the filters (ZL1 October 2012 and July 2013, and ZA  
165 July 2013) or from cell pellets obtained by centrifugation (ZA October 2012) using the

166 PowerWater® DNA Isolation Kit (Qiagen, Hilden, Germany) according to the manufacturer's  
167 instructions. Yield of DNA was determined using the QuBit® fluorometer (Invitrogen,  
168 Carlsbad, CA, United States) and the high sensitivity Assay Kit (Thermo Fisher Scientific,  
169 Waltham, MA, USA). For each sample, triplicate DNA extractions were performed from  
170 three of the six filters or pellets (the three other replicates were kept at -80°C as backup). The  
171 bacterial intergenic spacer regions between the small (16S) and the large (23S) subunits of  
172 ribosomal sequences were amplified from extracted DNA by PCR, using primers ITSF (5'-  
173 GTCGTAACAAGGTAGCCGTA-3') and ITSr (5'-GCCAAGGCATCCACC-3') [39]. For  
174 each of the eight samples, three independent PCR were performed on triplicate DNA extracts.  
175 PCR mix was prepared as follows: around 1 ng of DNA extract, 12 µl of amplitaq Gold 360  
176 master mix (Thermo Fisher Scientific), 2.5 µg of bovine serum albumin, and 0.5 µM of each  
177 primer, in a total volume of 25 µl. Cycling conditions were as previously described in [39].  
178 PCR products were checked on a 2% agarose gel. Then PCR products were analyzed on a  
179 microfluidic lab-on-a-chip (Agilent technologies, Santa Clara, United States). The lab-on-a-  
180 chip device is a fully automated electrophoresis system consisting of circuits of tiny closed  
181 channels and wells, etched onto a plastic microchip. Samples (PCR products) passed through  
182 selected pathways in a controlled manner. The DNA fragments (ranging between 263 and  
183 1500 bp depending on the bacterial taxa) were separated using the Agilent 2100 bioanalyser  
184 and the High Sensitivity DNA Analysis Kit. The fluorescence intensity was plotted versus the  
185 DNA fragment size and electropherograms corresponding to the band profiles characteristic  
186 of each bacterial community were edited with the Agilent 2100 bioanalyser software  
187 (including background noise removal). Then, three reproducible ARISA profiles were  
188 obtained for each water sample.

189 Data (expressed as peak size and peak area) were exported into Excel. One peak  
190 corresponds to one band on the profile (characterized by its size), and thus theoretically to one

191 bacterial phylotype present in the community; the area of the peak reflects the relative  
192 abundance of the corresponding phylotype inside the whole community. To take into account  
193 the variability of the technique, peak sizes (band sizes) were classified inside 10 pb-interval  
194 classes. A peak table was generated using the Agilent software for each triplicate.

195 Statistical analyses were performed using the free software R 3.4.3 ([http://www.r-](http://www.r-project.org/)  
196 [project.org/](http://www.r-project.org/), 2017). Nonmetric multidimensional scaling (NMDS) was used to graphically  
197 depict differences between the structures of the bacterial communities from the different  
198 samples (based on the normalized ARISA data expressed as the area of the peaks). The  
199 significance of the observed repartition of samples on the ordination plot was assessed by an  
200 ANalysis Of SIMilarity (ANOSIM, 999 permutations). To examine the relationships between  
201 bacterial structure communities and environmental variables, the main physico-chemical  
202 variables (temperature, pH, conductivity, redox potential, dissolved oxygen concentration and  
203 Total Organic Carbon concentration) were fitted onto NMDS. The environmental fitting (ef)  
204 model was tested with Monte Carlo permutation tests (999 randomized runs) to determine its  
205 significance. Plotting was limited to the most significant variables with argument  $p.max =$   
206  $0.05$  (after adjustment of the  $p$  values with the Banferroni correction). The length of the arrow  
207 is proportional to the correlation between the ordination of bacterial community structures and  
208 the environmental variable, called the strength of the gradient.

209

#### 210 2.4.2. *arsM* and *aioA* amplification, cloning and sequencing

211 For each of the eight samples, triplicate DNA extracts were pooled in equimolar  
212 proportions and PCR were performed on the eight DNA pools. Reactions, cycling conditions  
213 and primers for *arsM* gene amplification were previously described in [40]. For *aioA* gene  
214 amplification, primers aoxBM1-2F (5'-CCACTTCTGCATCGTGGGNTGYGGNTA-3') and

215 aoxBM3-2R (5'-TGTCGTTGCCCCAGATGADNCCYTTYT C-3') were used to amplify a  
216 1100 bp fragment [17]. The reaction contained 0.32  $\mu$ M of each primer, 10 ng of DNA  
217 extract, 1.5 mM MgCl<sub>2</sub>, 200  $\mu$ M of each deoxynucleoside triphosphate, 2.5 U of BIOTAQ™  
218 DNA polymerase (Eurobio, France) and 1X PCR buffer. Water was added to a final volume  
219 of 50  $\mu$ l. The PCR conditions included a 5 min denaturation step at 94°C, followed by 35  
220 cycles of a 45 s denaturation at 94°C, primer annealing of 45 s at 55°C, a 50 s extension at  
221 72°C, and a final extension at 72°C for 5 min. The *arsM* and *aioA* PCR products were  
222 visualized and purified after migration on an agarose gel using the Gel Band Purification Kit  
223 (GE-Healthcare, Munich, Germany).

224 *arsM* and *aioA* purified PCR products were cloned into a pCR® 2.1 vector and  
225 transformed into One Shot® TOP10 chemically Competent *Escherichia coli* TOP10 (Life  
226 Technologies, Carlsbad, CA) according to the protocols of the manufacturer. Twenty-seven to  
227 45 positive clones per library were sequenced by GATC biotech (Konstanz, Germany) with  
228 the M13 reverse primer. Nucleotide sequences were aligned with Muscle [41]. Conversion in  
229 protein sequences and phylogenetic analysis were carried out with the software MEGA6.06  
230 [42]. Amino acid sequences were compared with the GenBank database (NCBI) using  
231 BLAST [43]. Operational taxonomic units (OTUs) were determined using similarity levels  
232 between sequences of at least 80% of nucleotide similarity for *arsM* and 95% for *aioA* using  
233 Mothur v.1.33.2 [44]. Amino acid phylogenetic trees were constructed with a sequence  
234 representative of each OTU using the Maximum Likelihood method based on the LG model  
235 with 1000 bootstraps replicates. Initial tree(s) for the heuristic search were obtained by  
236 applying the Neighbor-Joining method to a matrix of pairwise distances estimated using a JTT  
237 model. A discrete Gamma distribution was used. The OTU-based DNA clustering data were  
238 also used to calculate rarefaction curves with R 3.6.0 to assess OTU richness from the  
239 different samplings.

240 2.4.3. *Sequence accession numbers*

241 The nucleotide and amino acid sequences reported in this article have been deposited  
242 in the GenBank database under the accession numbers API83135 to API83142.1 for *aioA* and  
243 API83143.1 to API83165.1 for *arsM*.

244

245 **3. Results**246 *3.1. Physico-chemical characterization of the lake waters*

247 The two lakes exhibited a water temperature in the range 19.8 – 25.7 °C (Table 1). The  
248 highest temperature was recorded at the surface of lake ZA in July 2013. The pH was slightly  
249 alkaline, from 8.5 to 8.9 in ZA and from 9.0 to 9.1 in ZL1. The two lakes were characterized  
250 by very high conductivity, particularly ZL1 (6.1 – 7.0 mS/cm in ZA; 14.5 – 15.5 mS/cm in  
251 ZL1). In lake ZA, redox potential (Eh) and dissolved oxygen concentration values (DO)  
252 revealed a redox gradient from the surface (DO = 9-11.5 mg/L, exceeded saturation in July  
253 2013; Eh = 360-400 mV) to the bottom (DO = 4-5 mg/L; Eh = 60-150 mV). Conversely,  
254 minor variations of DO and Eh occurred in lake ZL1 between the surface (DO=7.9-8.2 mg/L;  
255 Eh=312-336 mV) and the bottom (DO=8.3-9.2 mg/L; Eh=320-331 mV) whatever the  
256 sampling date. Total Organic Carbon concentration (TOC) was higher in ZA (~ 30-40 µg/L)  
257 than in ZL1 (~ 2-5 µg/L). The Chla concentration, measured in July 2013 at the surface, was  
258 higher in ZA (7 µg/L) than in ZL1 (< 1 µg/L).

259 Major ion concentrations revealed the Na-Cl-SO<sub>4</sub> facies of the lake waters (Table 1).  
260 The concentrations of these elements largely exceeded the regulation values for irrigation  
261 waters in the Moroccan legislation ([Na<sup>+</sup>] > 69 mg/L; [Cl<sup>-</sup>] > 350 mg/L; [SO<sub>4</sub><sup>2-</sup>] > 250 mg/L).  
262 Maximum arsenic concentrations reached 42 µg/L in ZA and 147 µg/L in ZL1. The values in  
263 ZL1 also exceeded Moroccan water quality standards for irrigation (100 µg/L). ZA was

264 characterized by the predominance of dimethylarsenic and As(V) (July 2013) or  
265 dimethylarsenic and As(III) (October 2012). However, DMA was not detected at the bottom  
266 of lake ZA in October 2012. In ZL1, As(V) was the only species detected (Table 1). Among  
267 other trace elements regulated for irrigation water, Li and Mo also exceeded Moroccan  
268 standards in ZA ( $[\text{Mo}] > 10 \mu\text{g/L}$ ) and ZL1 ( $[\text{Mo}] > 10 \mu\text{g/L}$ ;  $[\text{Li}] > 2500 \mu\text{g/L}$ ) (Table S1).

269

### 270 3.2. Whole bacterial community analysis

271 Whole bacterial community structure and its spatio-temporal variations were assessed  
272 by ARISA. The data, expressed as peak tables (deduced from ARISA electrophoregrams  
273 generated for each sample in triplicate), were used for NMDS analysis. The NMDS ordination  
274 shows that distinct bacterial communities thrived in waters from lakes ZL1 and ZA (ANOSIM  
275  $r^2 = 0.5845$ ,  $p = 0.001$ ; Fig. 2A). In lake ZL1, a limited spatio-temporal variability was  
276 observed among bacterial communities. In October 2012, the structures of the bacterial  
277 communities at the surface and at the bottom were undistinguishable. In contrast, marked  
278 temporal and spatial variations were observed in lake ZA. In particular, the bacterial  
279 communities sampled in October 2012 appeared widely different between surface and bottom.  
280 Vector fitting of possible explanatory environmental parameters revealed that conductivity  
281 (Cond), temperature ( $T^\circ$ ) and TOC contributed to the structuration of the bacterial  
282 communities in lake ZL1 and lake ZA. In ZL1, bacterial community structures were  
283 associated with a higher conductivity ( $r^2 = 0.7382$ ,  $p = 0.006$ ). In ZA, the structure of the  
284 communities was mainly associated to higher temperature ( $r^2 = 0.4322$ ,  $p = 0.006$ ) and TOC  
285 concentration ( $r^2 = 0.5364$ ,  $p = 0.012$ ) (Fig. 2A). On NMDS analysis based on data from lake  
286 ZA only, Eh ( $r^2 = 0.9768$ ,  $p = 0.006$ ), DO ( $r^2 = 0.9335$ ,  $p = 0.006$ ) and conductivity ( $r^2$   
287  $= 0.9934$ ,  $p = 0.006$ ) emerged as the main factors structuring the communities (Fig. 2B). Other

288 factors correlated with spatio-temporal changes in bacterial community structure were  
289 temperature ( $r^2 = 0.9316$ ,  $p = 0.006$ ) and TOC ( $r^2 = 0.9535$ ,  $p = 0.018$ ).

290

### 291 3.3. Arsenic methylating populations

292 No *arsM* amplification was obtained with DNA extracted from ZL1 water samples.  
293 *arsM* gene could be amplified from all the ZA samples except those collected at the bottom in  
294 July 2013. The *arsM* diversity was not entirely covered (rarefaction curves did not reach an  
295 asymptote), reflecting the important diversity of methylating bacteria in lake ZA (Fig. S1). A  
296 total of 22 OTUs were identified. In October 2012, the richness was slightly higher at the  
297 surface (13 OTUs) than at the bottom of the lake (8 OTUs). In July 2013, twelve OTUs were  
298 identified at the surface of the lake.

299 Phylogenetic analysis (performed with one representative sequence of each of the 22  
300 OTUs) showed a wide phylogenetic distribution of methylating bacteria in ZA (Fig. 3).  
301 Amino acid derived sequences were affiliated with ArsM sequences from Acidobacteria,  
302 Chloroflexi, Proteobacteria, Firmicutes, Bacteroidetes, Nitrospirales, Planctomycetes as well  
303 as uncultured environmental clones. Interestingly, the large majority (83 %) of the ArsM  
304 sequences from ZAbO12 grouped into five specific OTUs (containing no sequences from  
305 other samples). On the same way, 37% of the clones from ZAsO12 grouped into five specific  
306 OTUs. These observations suggest that distinct and specific methylating populations are  
307 thriving at the surface and at the bottom of this lake. No clear seasonal variations were  
308 observed for the distribution of *arsM* gene at the surface of the lake, suggesting these  
309 populations were stable over time. The most dominant OTU (represented by sequence  
310 ZAsJ13.23) contained sequences from all the ZA water samples (11% from ZAsO12, 3%  
311 from ZAbO12 and 58% from ZAsJ13). This OTU was affiliated (87% of amino acid

312 similarity) with the aerobic chemo-organotroph Acidobacteria *Bryobacter aggregatus* isolated  
313 from an acid peat soil [45]. The second most dominant and specific OTU (represented by  
314 sequence ZAbO12.22) contained 49% of the ZAbO12 sequences affiliated with a clone from  
315 a Chinese paddy soil contaminated with arsenic (90% of amino acid similarity) [46]. The third  
316 main OTU (represented by sequence ZAbO12.36) was also specific of the bottom of the lake  
317 (25% of the ZAbO12 library). This OTU was related to *Thermoflexus hugenholtzii* (80% of  
318 amino acid similarity), a thermophilic, heterotrophic microaerophilic and facultatively  
319 anaerobic bacterium isolated from sediment of Great Boiling Spring in Nevada [47]. Overall,  
320 few OTUs were closely related to any ArsM sequence from an isolated microorganism (Fig.  
321 3).

322

#### 323 3.4. Arsenite oxidizing populations

324 The *aioA* gene could be amplified only from ZL1sO12 and ZL1sJ13. The whole *aioA*  
325 diversity was covered (rarefaction curves reached an asymptote) for sample ZL1sO12 (Fig.  
326 S2), reflecting a low diversity of oxidizing microbial populations (4 OTUs). A higher richness  
327 (8 OTUs) was observed for sample ZL1sJ13.

328 The sequences from ZL1sO12 grouped into four OTUs that also contained sequences  
329 from July 2013. Other sequences from July 2013 grouped into four specific OTUs suggesting  
330 possible seasonal structuration of arsenite-oxidizing bacterial communities. The majority of  
331 the AioA sequences could not be related with confidence to any known organism, suggesting  
332 the presence in ZL1 of As(III) oxidizers not described yet. The two dominant OTUs were  
333 related to the putative AioA of the facultatively phototrophic *Rhodobacter capsulatus* (97%  
334 and 98% of amino acid similarity respectively) (Fig. 4).

335

## 4. Discussion

### 4.1. Arsenic speciation in the mine pit lakes

In lake ZL1, arsenic was present as inorganic As(V), whatever the season and the depth. This is consistent with the fully oxygenated conditions observed. Indeed, As(V) is the thermodynamically stable species in oxic conditions [48]. Arsenic speciation in ZL1 is consistent with other As-rich alkaline pit lakes in Canada and California where the shallow water depth favors oxygenated conditions and rapid oxidation of arsenite near the bottom sediment-water interface [49, 50]. In the present study, As(III) was not detected in lake ZL1. Thus, bacterially mediated reduction based on the *ars* detoxification system does not seem to contribute significantly to arsenic cycling in this lake. If dissimilarity As(V) reduction is not prone to occur in the oxygenated waters, such reductive process is not excluded in the anoxic sediments of the lake. Further characterization of the lake sediments would be required to determine if arsenic cycling in these pit lakes includes arsenate respiration as previously observed in sediments from a Mongolian soda lake [31].

In lake ZA, arsenic speciation was dominated by DMA. Several studies associated arsenic methylation in aquatic environments with phytoplankton development, linked to nutrient enrichment or seasonality (i.e light and temperature increase) [48, 51-52]. In the present study, ZA lake was characterized by a ten-fold higher TOC concentration as compared to lake ZL1. Moreover, the Chl<sub>a</sub> concentration (July 2013) was seven-fold higher in lake ZA (7 µg/L) than in lake ZL1 (1 µg/L). This suggests phytoplankton development and accumulation of organic matter in lake ZA. Tang et al. [53] recently demonstrated that anoxia induced by the degradation of algal biomass in freshwater promoted reduction and methylation of arsenic at the sediment/water interface, owing to the significant increase in arsenate reductase genes (*arrA* and *arsC*), and arsenite methyltransferase genes (*arsM*).

360 Although anoxia was not detected at the bottom of lake ZA, the DO decline from surface to  
361 bottom suggests that anoxia may occur in sediments, promoting microbial processes similar to  
362 those described by Tang et al. [53]. Thus, the presence of DMA in ZA might be linked to the  
363 eutrophic character of this lake. The high productivity of lake ZA may be favored by the  
364 erosion and leaching of nutrients from the ore flotation residues originating from the Zeida  
365 ore treatment facility, stored next to the lake. Indeed, the phosphorus content of these residues  
366 (1.77 %, [3]) is higher than the average content in soil (0.6 %) and they contain fine particles  
367 (50 % of particles with size lower than 0.2 mm, [3]), propitious for phosphorous leaching.  
368 DMA co-existed either with As(III) (October 2012) or with As(V) (July 2013) in ZA lake.  
369 However, DMA was not detected at the bottom of ZA in July 2013. Seasonal differences  
370 observed in arsenic speciation in ZA lake remains unexplained and a more comprehensive  
371 view of arsenic cycling in these pit lakes would require further investigations.

372

#### 373 *4.2. Microbial contribution to arsenic biogeochemical cycling in Moroccan pit lakes*

374 A recent study investigated bacterial diversity in a meromictic pit lake where arsenic  
375 was present under the forms As(III) and As(V) depending on the redox conditions. Bacterial  
376 genera including potential As(III) oxidizers and As(V) reducers were identified although  
377 functional genes involved in arsenic biotransformation were not investigated [54]. Arsenic  
378 biogeochemistry has been studied in highly saline soda lakes originating from geothermal  
379 water input in California [55, 56] and Mongolia [31]. Soda lakes exhibit considerably higher  
380 As concentrations (~ 15 mg As/L) and salinity (70 to 90 g/L) compared to lakes ZL1 and ZA,  
381 but similar pH (pH 9.8). Arsenic speciation in soda lakes is dominated by inorganic As(III)  
382 and As(V) species [55]. Arsenic oxidation in Mono Lake is mediated by bacteria and is  
383 coupled to the reduction of nitrate rather than oxygen. Although both *aioA* and *arxA*  
384 transcripts were detected in Mono Lake transcriptome, As(III) oxidation appeared to be

385 predominantly catalysed by ArxA under anoxic conditions [57]. In the present study, the  
386 detection of *aioA* gene in ZL1, together with the presence of As(V), suggests that aerobic  
387 bacterial arsenite oxidation occurred in this pit lake. However, arsenic might be released from  
388 the lake walls in the form of As(V). Furthermore, considering the oxygenated conditions of  
389 lake ZL1 whatever the season and depth, abiotic As(III) oxidation, although being a slow  
390 process, may not be excluded. Further investigations based on the expression of *aioA* would  
391 be necessary to conclude if bacterial oxidation actually occurs in ZL1. Because it is not  
392 possible to infer phylogenetic relationships based on *aioA* gene, the identity of the potential  
393 arsenite oxidizers remains unknown. The fact that *aioA* amplification failed for ZA lake  
394 samples doesn't necessarily reflect the absence of arsenite oxidizers. They may be present in  
395 very low proportions or they may not be targeted by the primers used in this study.

396 Contrary to ZL1, arsenic in ZA was predominantly in the methylated form (DMA). A  
397 wide range of prokaryotic and eukaryotic microorganisms (bacteria, archaea, algae, and fungi)  
398 has the capacity to methylate arsenic [19], including photosynthetic organisms [58].  
399 Furthermore, complex organoarsenic compounds such as arsenosugars are produced by  
400 diverse organisms including algae, bacteria, and fungi [59]. Methyl arsenic species may  
401 originate from the degradation of such organic compounds by bacterial activity (as shown for  
402 seawater bacteria degrading arsenobetaine, [60]). However, our results clearly showed that the  
403 genetic potential for bacterially mediated arsenic methylation (*arsM* gene) is phylogenetically  
404 diverse and widely distributed in ZA waters. This strongly suggests that bacterial activity  
405 plays a direct role in the production of DMA in this lake. Environmental diversity surveys of  
406 *arsM* gene on aquatic environments are scarce. An unexpected diversity of bacteria with the  
407 genetic potential for arsenic methylation was also evidenced in a river impacted by acid mine  
408 drainage [40]. Conversely, arsenic methylation activity was not evidenced in Mono Lake,  
409 contrary to other arsenic-related functions [57]. Recently, Tang et al. [53] demonstrated in

410 laboratory experiments that organic carbon enriched anoxic environments promoted the  
411 growth of arsenite methylating bacteria, leading to enhanced formation of methylated arsenic  
412 at the sediment/water interface. To our knowledge, the present work is the first report of  
413 methylated forms of arsenic associated with the presence of methylating bacteria in an  
414 alkaline pit lake. Similarly to *aioA*, *arsM* phylogeny does not allow to infer taxonomic  
415 identification of the corresponding bacteria. However, our findings strengthen the idea that  
416 bacterially mediated arsenic methylation may contribute to the global As biogeochemical  
417 cycle in freshwater ecosystems [40, 61]. A prominent role of biomethylation in soils was also  
418 recently suggested, based on the unexpected abundance of *arsM* in soil metagenomes [62].

419

#### 420 *4.3. Physico-chemical drivers of bacterial communities*

421 ARISA fingerprinting showed that the structure of the whole bacterial community  
422 differed between the two lakes. The main parameters that shaped these communities were  
423 conductivity, TOC and temperature. Salinity (i.e. conductivity) can indeed strongly control  
424 microbial community composition [63, 64]. In freshwater reservoirs, organic carbon  
425 concentration appeared an important driver of the bacterial community composition, besides  
426 pH and alkalinity [65]. Thus, the contrasting values of conductivity, total organic carbon  
427 concentration and temperature in lakes ZA and ZL1 probably selected distinct bacterial  
428 populations. The study of the marker genes involved in As biotransformations points to the  
429 same conclusion. Indeed, a high diversity of bacteria with the *arsM* gene was recovered in  
430 lake ZA while this gene was not detected in lake ZL1. Conversely, *aioA* gene was amplified  
431 only in lake ZL1. This suggests that distinct bacterial groups were involved in the As cycle in  
432 ZA and in ZL1.

433 In lake ZL1, the spatio-temporal variations of the whole bacterial community as well  
434 as of the arsenite oxidizing populations were limited. This is in agreement with the narrow  
435 range of variations highlighted for the water physico-chemical conditions. On the contrary, in  
436 the stratified ZA lake, pronounced changes in bacterial community structure and *ArsM*  
437 diversity were associated with marked spatio-temporal variations of the water physico-  
438 chemistry. Eighty three percent of *ArsM* sequences recovered at the bottom of ZA lake were  
439 not recovered in the surface waters (Fig.3). This may be explained by the drastic change in  
440 DO and Eh between surface (DO = 8.7-11.5 mg/L, Eh = 361-399 mV) and bottom (DO = 4.1-  
441 4.8 mg/L, Eh = 61-153 mV) waters. Reducing conditions generated near the sediment/water  
442 interface may have selected specific bacterial populations involved in As methylation [53].  
443 Moreover, the dominant OTU containing 58% of the *arsM* sequences retrieved from surface  
444 waters in July 2013 represented only 10% of the whole *arsM* sequences in October 2012 (Fig.  
445 3). This suggests a seasonal dynamic of the bacterial populations involved in As methylation  
446 in lake ZA. This dynamic can be related to seasonal change of TOC, temperature or DO  
447 (Table 1). The physico-chemical drivers structuring the bacterial community carrying As  
448 transforming genes are poorly documented in the literature. In soils contaminated with arsenic  
449 [46, 66], the most important factors shaping As transformation functional genes were soil pH,  
450 phosphate-extractable As, and amorphous Fe content [66]. Total C and N also drove the  
451 variation in gene abundance and microbial community associated with As biotransformation  
452 [46]. Further work is necessary to decipher the physico-chemical parameters shaping the  
453 bacterial diversity involved in As biotransformation (methylation, oxidation) in alkaline pit  
454 lakes.

#### 455 4.4. Environmental significance

456 Arsenic biotransformations have been overlooked so far for moderately saline alkaline pit  
457 lakes which are potentially important freshwater resources in semi-arid Mediterranean areas.

458 In the present study, there is a body of evidence that the bacterial communities inhabiting  
459 such pit lakes are contributing to As biogeochemical cycling. The eutrophic or oligotrophic  
460 status of the pit lakes and the salinity appeared to be important drivers of the As-oxidizing and  
461 As-methylating bacterial populations. Arsenic biomethylation evidenced in lake ZA may  
462 contribute to attenuate the toxicity of arsenic compared to lake ZL1 where no methylation  
463 occurs [21]. However, the possible presence of toxic volatile forms should be assessed since  
464 they may represent a threat for public health [53]. Furthermore, other elements such as Mo  
465 and Li compromise the use of this resource for irrigation [3].

466

## 467 5. Conclusion

468 Here we report for the first time arsenic speciation and As-related bacterial genes diversity  
469 in Moroccan alkaline mine pit lakes. The first outcome is the contrasting arsenic speciation in  
470 the two pit lakes that may be explained by the different content in organic carbon. Indeed,  
471 high organic carbon concentration in ZA was associated with a redox and DO gradient while  
472 lake ZL1, characterized by lower organic carbon content, showed no stratification. In lake  
473 ZA, the high TOC content is probably an important factor associated with biomethylation  
474 activity and the presence of diverse *arsM*-carrying bacteria. In lake ZL1, fully oxygenated  
475 conditions involved the predominance of As(V), in agreement with thermodynamic  
476 predictions. Bacterial populations carrying the *aioA* gene were evidenced in lake ZL1,  
477 suggesting that biotic As(III) oxidation may occur. For a more comprehensive view of arsenic  
478 cycling in these lakes, further work should focus on arsenic speciation and bacterial diversity  
479 at the sediment/water interface of the lake where reductive conditions are prone to favor  
480 As(V) reduction and biomethylation.

481

482 **Conflict of interest**

483 Authors declare no conflict of interest.

484

Journal Pre-proof

485 **Acknowledgements:**

486 The authors thank Vincent Tardy for his help with statistical analyses. We thank Pr  
487 Mohammed Rouai for his help on the field. The authors thank the Cooperation program  
488 “Convention d’échanges” CNRS/CNRST Maroc (2012-2013) and the Sicmed network “  
489 Activités minières dans le bassin méditerranéen – Interactions contaminants métalliques /  
490 écosystèmes - interfaces avec la santé, l’environnement et la société.

491

492

Journal Pre-proof

493 **References**

- 494 [1] Smedley P, Kinniburgh D. A review of the source, behaviour and distribution of arsenic in  
495 natural waters. *Appl Geochem* 2002;17:517–68.
- 496 [2] EL Hachimi ML, EL Hanbali M, Fekhaoui M, Bouabdli A, EL Founti L, Saïdi N. Impact  
497 d'un site minier abandonné sur l'environnement: cas de la mine de Zeïda (Haute  
498 Moulouya, Maroc). *Bull de l'institut Sci Rabat Sect Sci Terre* 2005;93–100.
- 499 [3] EL Hachimi ML, Bouabdli A, Fekhaoui M. Les rejets miniers de traitement :  
500 caractérisation, capacité polluante et impacts environnementaux, mine Zeïda, mine  
501 Mibladen, Haute Moulouya (Maroc). *Déchets Sciences et Techniques* 2013;32–45.
- 502 [4] Iavazzo P, Ducci D, Adamo P, Trifuoggi M, Migliozzi A, Boni M. Impact of past mining  
503 activity on the quality of water and soil in the High Moulouya Valley (Morocco).  
504 *Water Air Soil Pollut* 2012;223:573–89.
- 505 [5] Metallogenic Map of Europe and neighbouring countries. Prof. Gunnar Juve (NGU-  
506 Norway), CGMW-Geological Survey of Norway (NGU) co-edition. 1997. Available  
507 at : <http://ccgm.org/en/catalogue/121-carte-metallogenique-de-l-europe.html>
- 508 [6] Fuller CC and Davis JA. Influence of coupling of sorption and photosynthetic processes  
509 on trace element cycles in natural waters. *Nature* 1989;340:52-54.
- 510 [7] Eary LE. Geochemical and equilibrium trends in mine pit lakes. *Appl Geochem* 1999;14:  
511 963–87.
- 512 [8] Mukhopadhyay R, Rosen BP, Phung LT, Silver S. Microbial arsenic: from geocycles to  
513 genes and enzymes. *FEMS Microbiol Rev* 2002, 26 :311–325
- 514 [9] Bruneel O, Héry M, Laroche E, Dahmani I, Fernandez-Rojo L, Casiot C. “Microbial  
515 transformations of arsenic: from metabolism to bioremediation,” in *Metal-microbe*  
516 *Interactions and Bioremediation: Principle and Applications for Toxic Metals*, 2017,  
517 eds S. Das and H. R. Dash (CRC Press: Abingdon).

- 518 [10] Zhu YG, Xue XM, Kappler A, Rosen BP, Meharg AA. Linking Genes to Microbial  
519 Biogeochemical Cycling: Lessons from Arsenic. *Environ Sci Technol* 2017 ; 51(13) :  
520 7326-7339
- 521 [11] Santini JM, Sly LI, Schnagl RD, Macy JM. A new chemolithoautotrophic arsenite-  
522 oxidizing bacterium isolated from a gold mine: phylogenetic, physiological, and  
523 preliminary biochemical studies. *Appl Environ Microbiol* 2000;66:92–97.
- 524 [12] Duquesne K, Lieutaud A, Ratouchniak J, Muller D, Lett MC, Bonnefoy V. Arsenite  
525 oxidation by a chemoautotrophic moderately acidophilic *Thiomonas* sp.: from the  
526 strain isolation to the gene study. *Environ Microbiol* 2008;10:228–37.
- 527 [13] Stolz JF, Basu P, Oremland RS. Microbial arsenic metabolism: New twists on an old  
528 poison: During the early anoxic phase on Earth, some microbes depended on arsenic  
529 to respire. *Microbe Mag* 2010;5:53–9.
- 530 [14] Andreoni V, Zanchi R, Cavalca L, Corsini A, Romagnoli C, Canzi E. Arsenite oxidation  
531 in *Ancylobacter dichloromethanicus* As3-1b strain: detection of genes involved in  
532 Arsenite oxidation and CO<sub>2</sub> fixation. *Curr Microbiol* 2012;65:212–18.
- 533 [15] Anderson GL, Williams J, Hille R. The purification and characterization of Arsenite  
534 oxidase from *Alcaligenes faecalis*, a molybdenum-containing hydroxylase. *J Biol*  
535 *Chem* 1992;267(33):23674-82267.
- 536 [16] Inskeep WP, Macur RE, Hamamura N, Warelow TP, Ward SA, Santini JM. Detection,  
537 diversity and expression of aerobic bacterial arsenite oxidase genes. *Environ*  
538 *Microbiol* 2007;9:934–943.
- 539 [17] Quemeneur M, Heinrich-Salmeron A, Muller D, Lievremont D, Jauzein M, Bertin PN,  
540 et al. Diversity surveys and evolutionary relationships of *aoxB* genes in aerobic  
541 arsenite-oxidizing bacteria. *Appl Environ Microbiol* 2008;74:4567–73.

- 542 [18] Zargar K, Hoefl S, Oremland RS, and Saltikov CW. Identification of a novel arsenite  
543 oxidase gene *arxA*, in the haloalkaliphilic, arsenite-oxidizing bacterium  
544 *Alkalilimnicola ehrlichii* strain MLHE-1. *J Bacteriol* 2010;192:3755–62.
- 545 [19] Bentley R, Chasteen TG. Microbial Methylation of Metalloids: Arsenic, Antimony, and  
546 Bismuth. *Microbiol mol biol reviews* 2002;66(2):250–271
- 547 [20] Yin XX, Chen J, Qin J, Sun GX, Rosen BP, Zhu YG. Biotransformation and  
548 volatilization of arsenic by three photosynthetic *Cyanobacteria*. *PLANT Physiol*  
549 2011;156:1631–38.
- 550 [21] Styblo M, Del Razo LM, Vega L., Germolec DR, LeCluyse EL, Hamilton GA, Reed W,  
551 Wang C, Cullen WR, Thomas DJ. Comparative toxicity of trivalent and pentavalent  
552 inorganic and methylated arsenicals in rat and human cells. *Arch Toxicol* 2000 ;  
553 74(6):289–299
- 554 [22] Qin J, Rosen BP, Zhang Y, Wang G, Franke S, Rensing C. Arsenic detoxification and  
555 evolution of trimethylarsine gas by a microbial arsenite S-adenosylmethionine  
556 methyltransferase. *Proc Natl Acad Sci USA* 2006;103(7):2075-80.
- 557 [23] Dopp E, Kligerman AD, Diaz-Bone RA. Organoarsenicals. Uptake, metabolism, and  
558 toxicity. *Metal Ions in Life Sciences* 2010a;7: 231–265.
- 559 [24] Dopp E, von Recklinghausen U, Diaz-Bone R, Hirner AV, Rettenmeier AW. Cellular  
560 uptake, subcellular distribution and toxicity of arsenic compounds in methylating and  
561 non-methylating cells. *Environmental Research* 2010b; 110: 435–442.
- 562 [25] Oremland RS, Stolz JF. The ecology of arsenic. *Science* 2003; 300(5621):939-44.
- 563 [26] Kumarathilaka P, Seneweera S, Meharg A, Bundschuh J. Arsenic speciation dynamics in  
564 paddy rice soil-water environment: sources, physico-chemical, and biological factors -  
565 A review. *Water Res* 2018; 140:403-414

- 566 [27] Andreae MO. Distribution and speciation of arsenic in natural waters and some marine  
567 algae. *Deep Sea Research* 1978;25(4):391-402.
- 568 [28] Andreae MO. Arsenic speciation in seawater and interstitial waters : the influence of  
569 biological-chemical interactions on the chemistry of a trace element. *Limnol and*  
570 *Oceanogr* 1979 ; 24 (3) : 440-452.
- 571 [29] Cui J and Jing C. A review of arsenic interfacial geochemistry in groundwater and the  
572 role of organic matter. *Ecotoxicol Environ Saf* 2019 ; 83:109550
- 573 [30] Sorokin DY, Berben T, Melton ED, Overmars L, Vavourakis CD, Muyzer G. Microbial  
574 diversity and biogeochemical cycling in soda lakes. *Extremophiles* 2014 ; 18:791–809
- 575 [31] Hamamura N, Itai T, Liu Y, Reysenbach AL, Damdinsuren N, Inskeep WP.  
576 Identification of anaerobic arsenite-oxidizing and arsenate-reducing bacteria  
577 associated with an alkaline saline lake in Khovsgol, Mongolia. *Environmental*  
578 *Microbiology Reports* 2014; 6(5): 476–48
- 579 [32] Doumas P, Munoz M, Banni M, Becerra S, Bruneel O, Casiot C, Cleyet-Marel JC,  
580 Gardon J, Noak Y, Sappin-Didier V. Polymetallic pollution from abandoned mines in  
581 Mediterranean regions: a multidisciplinary approach to environmental risks. *Regional*  
582 *Environmental Change* 2018 ;18(3) : 677–692
- 583 [33] Ranjard L, Nazaret S, Gourbière F, Thioulouse J, Linet P, Richaume A. A soil microscale  
584 study to reveal the heterogeneity of Hg(II) impact on indigenous bacteria by  
585 quantification of adapted phenotypes and analysis of community DNA fingerprints.  
586 *FEMS Microbiol Ecol* 2000; 31:107–115.
- 587 [34] van Dorst J, Bissett A, Palmer AS, Brown M, Snape I, Stark JS, Raymond B, McKinlay  
588 J, Ji1 M, Winsley T, Ferrari BC. Community fingerprinting in a sequencing world.  
589 *FEMS Microbiol Ecol* 2014 ; 1–15

- 590 [35] EL Hachimi ML. Les districts miniers Aouli- Mibladen-Zeïda, abandonnés dans la Haute  
591 Moulouya (Maroc): potentiel de pollution et impact sur l'environnement. 2006. Thèse  
592 de Doctorat. Université IBN Tofail, Kénitra.
- 593 [36] Amade E. Les gisements de plomb de Zeïda et de Boumia. Colloque sur des gisements  
594 stratiformes de plomb, zinc et de manganèse du Maroc. Notes Mém Serv Géol. 1965;  
595 n°181:175 - 84.
- 596 [37] Casiot C, Egal M, Elbaz-Poulichet F, Bruneel O, Bancon-Montigny C, Cordier MA, et  
597 al. Hydrological and geochemical control of metals and arsenic in a Mediterranean  
598 river contaminated by acid mine drainage (the Amous River, France); preliminary  
599 assessment of impacts on fish (*Leuciscus cephalus*). *Appl Geochem* 2009;24:787–99.
- 600 [38] Halter D, Casiot C, Simon S, Heipieper HJ, Marchal M, Lièvremon D, et al. Surface  
601 properties and intracellular speciation revealed an original adaptive mechanism to  
602 arsenic in the acid mine drainage bio-indicator *Euglena mutabilis*. *Appl Microbiol*  
603 *Biotechnol* 2012; 93(4):1735-44.
- 604 [39] Cardinale M, Brusetti L, Quatrini P, Borin S, Puglia AM, Rizzi A, et al. Comparison of  
605 different primer sets for use in Automated Ribosomal Intergenic Spacer Analysis of  
606 complex bacterial communities. *Appl Environ Microbiol* 2004;70:6147–56.
- 607 [40] Desoeuvre A, Casiot C, Héry M. Diversity and distribution of arsenic-related genes along  
608 a pollution gradient in a river affected by acid mine drainage. *Microb Ecol* 2016;71:  
609 672–85.
- 610 [41] Edgar RC. MUSCLE: a multiple sequence alignment method with reduced time and  
611 space complexity. *BMC Bioinformatics* 2004;5:113.
- 612 [42] Tamura K, Stecher G, Peterson D, Filipski A, Kumar S. MEGA6: Molecular  
613 evolutionary genetics analysis version 6.0. *Mol Biol Evol* 2013;30: 2725–29.

- 614 [43] Altschul SF, Gish W, Miller W, Myers EW, Lipman DJ. Basic Local Alignment Search  
615 Tool J Mol Biol 1990;215(3):403–10.
- 616 [44] Schloss PD, Westcott SL, Ryabin T, Hall JR, Hartmann M, Hollister EB et al.  
617 Introducing mothur: open-source, platform-independent, community-supported  
618 software for describing and comparing microbial communities. Appl Environ  
619 Microbiol 2009;75:7537–41.
- 620 [45] Kulichevskaya IS, Suzina NE, Liesack W, Dedysh SN. *Bryobacter aggregatus* gen. nov.,  
621 sp. nov., a peat-inhabiting, aerobic chemo-organotroph from subdivision 3 of the  
622 Acidobacteria. IJSEM 2010;60:301–06.
- 623 [46] Zhang SY, Zhao FJ, Sun GX, Su JQ, Yang XR, Li H, et al. Diversity and abundance of  
624 arsenic biotransformation genes in paddy soils from southern China. Environ Sci  
625 Technol 2015;49:4138–46.
- 626 [47] Dodsworth JA, Gevorkian J, Despujos F, Cole JK, Murugapiran SK, Ming H, et al.  
627 *Thermoflexus hugenholtzii* gen. nov., sp. nov., a thermophilic, microaerophilic,  
628 filamentous bacterium representing a novel class in the *Chloroflexi*, *Thermoflexia*  
629 *classis* nov., and description of *Thermoflexaceae* fam. nov. and *Thermoflexales* ord.  
630 nov. IJSEM 2014;64(6): 2119-27
- 631 [48] Hasegawa H, Rahman MA, Kitahara K, Itaya Y, Maki T, Ueda K. Seasonal changes of  
632 arsenic speciation in lake waters in relation to eutrophication. Sci Total Environ  
633 2010;408:1684–90.
- 634 [49] Martin AJ, Pedersen TF. Seasonal and interannual mobility of arsenic in a lake impacted  
635 by metal mining. Environ Sci Technol 2002;36:1516–23.
- 636 [50] Savage KS, Ashley RP, Bird DK. Geochemical evolution of a high arsenic, alkaline pit-  
637 lake in the Mother Lode Gold District, California. Econ Geol 2009;104:1171–1211.

- 638 [51] Hasegawa H, Rahman MA, Matsuda T, Kitahara T, Maki T, Ueda K. Effect of  
639 eutrophication on the distribution of arsenic species in eutrophic and mesotrophic  
640 lakes. *Sci Total Environ* 2009; 407: 1418–1425
- 641 [52] Rahman MA, Hasegawa H. Arsenic in freshwater systems: Influence of eutrophication  
642 on occurrence, distribution, speciation, and bioaccumulation. *Appl Geochem*  
643 2012;27:304–14.
- 644 [53] Tang Y, Zhang M, Sun G, Pan G. Impact of eutrophication on arsenic cycling in  
645 freshwaters. *Water Res* 2019 ; 150 : 191-199.
- 646 [54] von Gunten K, Warchola T, Donner MW, Cossio M, Hao W, Boothman C, et al.  
647 Biogeochemistry of U, Ni, and As in two meromictic pit lakes at the Cluff Lake  
648 uranium mine, northern Saskatchewan. *Can J Earth Sci* 2018;55:463–74.
- 649 [55] Oremland RS, Stolz JF, Hollibaugh JT. The microbial arsenic cycle in Mono Lake,  
650 California. *FEMS Microbiol Ecol* 2004;48:15–27.
- 651 [56] Oremland RS, Saltikov CW, Stolz JF, Hollibaugh JT. Autotrophic microbial  
652 arsenotrophy in arsenic-rich soda lakes. *FEMS Microbiol Lett* 2017;364.
- 653 [57] Edwardson CF and Hollibaugh JT. Metatranscriptomic analysis of prokaryotic  
654 communities active in sulfur and arsenic cycling in Mono Lake, California, USA *The*  
655 *ISME J* 2017;11:2195–208
- 656 [58] Ye J, Rensing C, Rosen BP, Zhu YG. Arsenic biomethylation by photosynthetic  
657 organisms. *Trends Plant Sci* 2012; 17(3):155-62.
- 658 [59] Francesconi KA, Kuehnelt D. Arsenic compounds in the environment in *Environmental*  
659 *Chemistry of Arsenic* (Ed. W. T. Frankenberger, Jr) 2002, pp. 51–94 (Marcel Dekker  
660 Inc.: New York).
- 661 [60] Hanaoka K, Nakamura O, Ohno H, Tagawa S, Kaise T. Degradation of arsenobetaine to  
662 inorganic arsenic by bacteria in seawater. *Hydrobiologia* 1995 ; 316(1) : 75–80

- 663 [61] Héry M, Casiot C, Resongles E, Gallice Z, Bruneel O, Desoeuvre A, et al. Release of  
664 arsenite, arsenate and methyl-arsenic species from streambed sediment affected by  
665 acid mine drainage: a microcosm study. *Environ Chem* 2014;11:514.
- 666 [62] Dunivin TK, Yeh SY, Shade A. A global survey of arsenic-related genes in soil  
667 microbiomes. *BMC Biology* 2019 ; 17: 45
- 668 [63] Lozupone CA, Knight R. Global patterns in bacterial diversity. *Proc Natl Acad Sci*  
669 2007;104:11436–40.
- 670 [64] Auguet JC, Barberan A, Casamayor EO. Global ecological patterns in uncultured  
671 Archaea. *ISME J* 2010;4:182–90.
- 672 [65] Llíros M, Inceoğlu Ö, García-Armisen T, Anzil A, Leporcq B, Pigneur LM, et al.  
673 Bacterial community composition in three freshwater reservoirs of different alkalinity  
674 and trophic status. *PLoS ONE* 2014;9:e116145.
- 675 [66] Gu Y, Van Nostrand JD, Wu L, He Z, Qin Y, Zhao FJ et al. Correction: Bacterial  
676 community and arsenic functional genes diversity in arsenic contaminated soils from  
677 different geographic locations. *PLoS ONE* 2017;12:e0189656.
- 678
- 679
- 680
- 681
- 682
- 683
- 684
- 685

686 **Legends to figures**

687 **Figure 1.** General map of the study area (A) showing mine pit lakes ZA and ZL1, located  
688 north and south from the town of Zeida (or Zaida), closed to the Moulouya River (B).  
689 Situation of lake ZA closed to ore treatment residues (C) and lake ZL1 surrounded by tailings  
690 piles (D). Water sampling stations are indicated by a red star. Adapted from Google Maps and  
691 Google Earth.

692  
693 **Figure 2.** Nonmetric multidimensional scaling (NMDS) ordination plots derived from  
694 weighted pairwise Unifrac distances for bacterial communities structure (ARISA) for all  
695 samples (A) or samples from lake ZA only (B). Stress values for ordination plot are  $< 0.2$   
696 which indicates that these data are well-represented by the two-dimensional representation.  
697 Environmental fitting is based on the main physico-chemical parameters ( $T^{\circ}$ : temperature;  
698 pH; Cond: conductivity; Eh: redox potential; DO: dissolved oxygen concentration; TOC: total  
699 organic carbon concentration). The full and dotted arrows represent significant and non-  
700 significant fittings, respectively (Bonferroni corrected,  $p < 0.05$ ).

701 **Figure 3:** ArsM phylogenetic tree based on 112 to 157 AA sequences using the Maximum  
702 Likelihood method. ArsM sequences (in bold) are representative sequences of each OTUs  
703 based on a 80% nucleotide sequence similarity cut-off. For each of the three clone libraries,  
704 the percentage of clones contained in each OTU is indicated in brackets.

705  
706 **Figure 4:** AioA phylogenetic tree based on 242 to 265 AA sequences using the Maximum  
707 Likelihood method. AioA sequences (in bold) are representative sequences of each OTUs  
708 based on a 95% nucleotide sequence similarity cut-off. For each clone libraries, the  
709 percentage of clones contained in each OTU is indicated in brackets

710

## Supplementary material

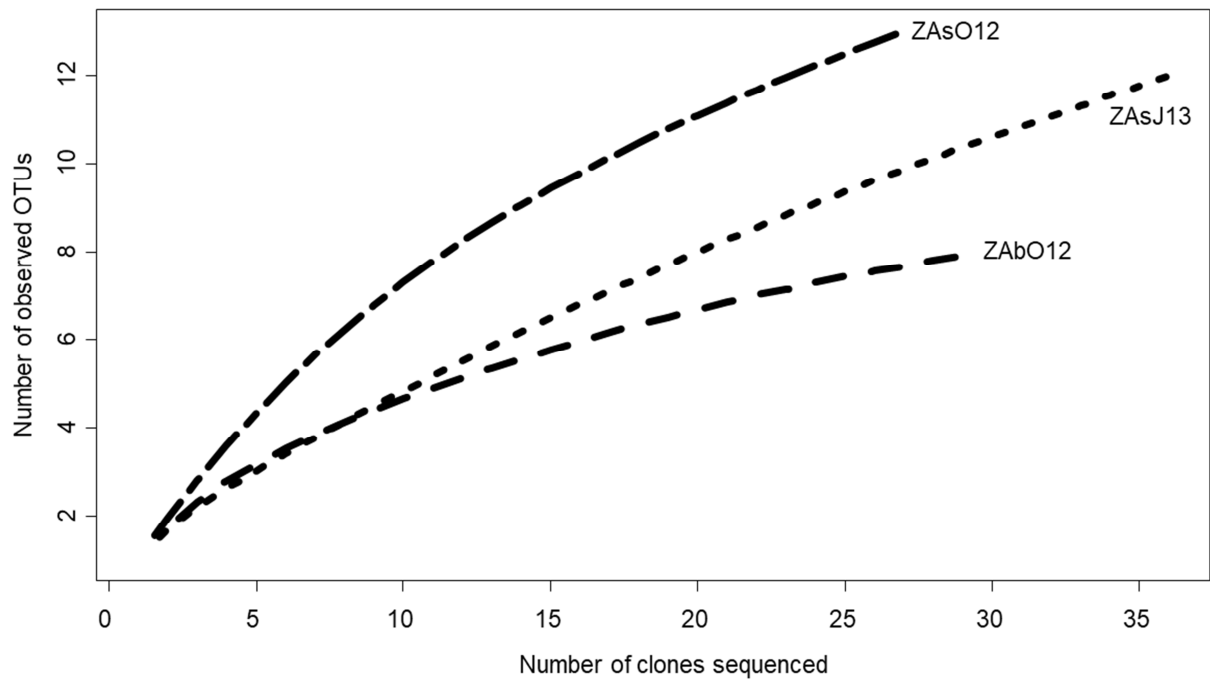
711 **Table S1** - Concentrations of trace elements at the surface and at the bottom of lakes ZA and  
 712 ZL1 in October 2012 and July 2013

Parameter ( $\mu\text{g/L}$ )	ZA lake				ZL1 Lake			
	October-2012		July-2013		October-2012		July-2013	
	surface	bottom(5 m)	surface	bottom(5 m)	surface	bottom(12.5 m)	surface	bottom(12.5 m)
Li	924	922	2296	2282	4502	4450	11400	10870
B	985	1009	980	997	2586	2539	2600	2479
Al	15.2	39.6	25.0	32.1	<DL	<DL	37.0	25.0
Si	<DL	<DL	2025	3017	<DL	<DL	16420	16120
Ti	<DL	<DL	1.6	2.1	<DL	<DL	7.1	6.0
V	5.1	5.3	2.8	2.5	15.7	15.5	17.3	16.6
Cr	<DL	<DL	0.2	0.2	<DL	<DL	0.8	0.9
Mn	66.8	78.6	6.6	46.2	5.3	4.1	7.9	8.1
Fe	22.2	18.8	32.4	40.9	<DL	<DL	31.2	32.0
Co	0.6	0.6	0.5	0.6	<DL	0.3	0.2	0.2
Ni	1.6	1.5	2.2	2.1	<DL	<DL	1.3	1.3
Cu	1.2	<DL	3.0	2.6	<DL	<DL	2.9	<DL
Zn	11.5	7.7	5.6	61.6	<DL	26.9	28.9	<DL
Se	0.5	n.d.	0.4	0.2	4.6	9.1	6.4	3.8
Rb	34.5	36.5	33.8	35.4	248.9	248.3	256.3	246.4
Sr	1300	1362	3961	4061	1672	1663	4730	4564
Mo	21.0	18.7	28.2	26.8	260.7	263.4	262.5	251.5
Ag	<DL	<DL	5.5	<DL	<DL	<DL	<DL	<DL
Cd	0.1	0.1	0.1	0.1	0.7	0.6	0.6	0.7
Sb	3.1	2.5	2.0	1.5	2.4	2.2	2.4	2.0
Cs	0.3	0.3	0.3	0.3	4.1	4.1	3.5	3.5
Ba	41.5	40.3	29.9	30.6	83.3	82.7	86.9	81.2
Tl	0.0	0.0	0.5	0.0	0.1	0.0	0.0	0.0
Pb	16.1	9.2	8.1	6.1	10.9	3.7	11.6	6.4
U	31.9	30.9	29.0	27.8	321.2	319.0	308.9	300.1

713  
 714 n.d. = not determined; <DL = below detection limit

715

716



717

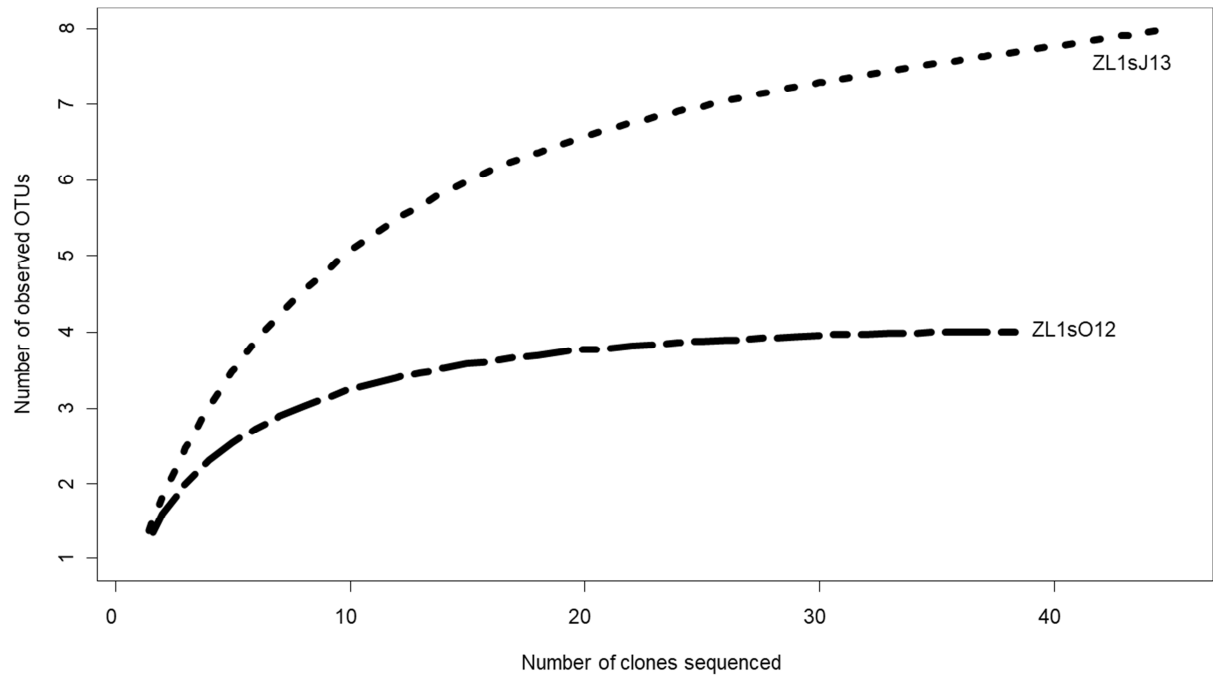
718 **Figure S1:** Rarefaction curves of *arsM* gene for the ZA libraries. The total number of

719 sequences analyzed is plotted against the number of OTUs observed in the same library.

720

721

722



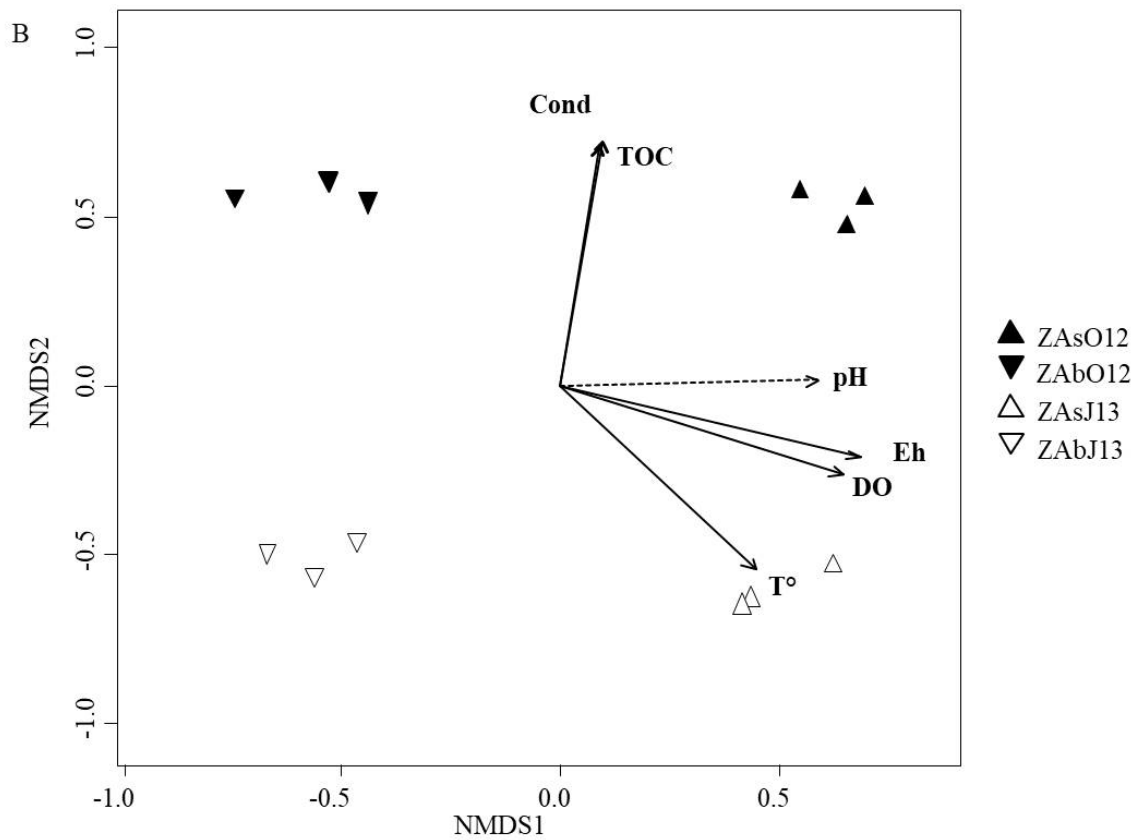
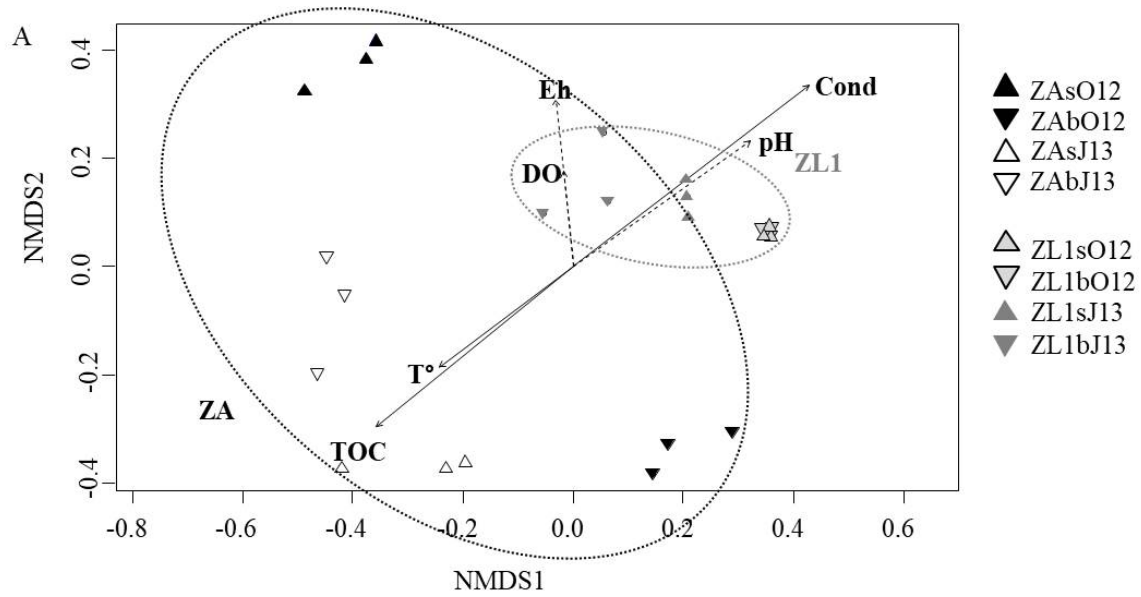
723

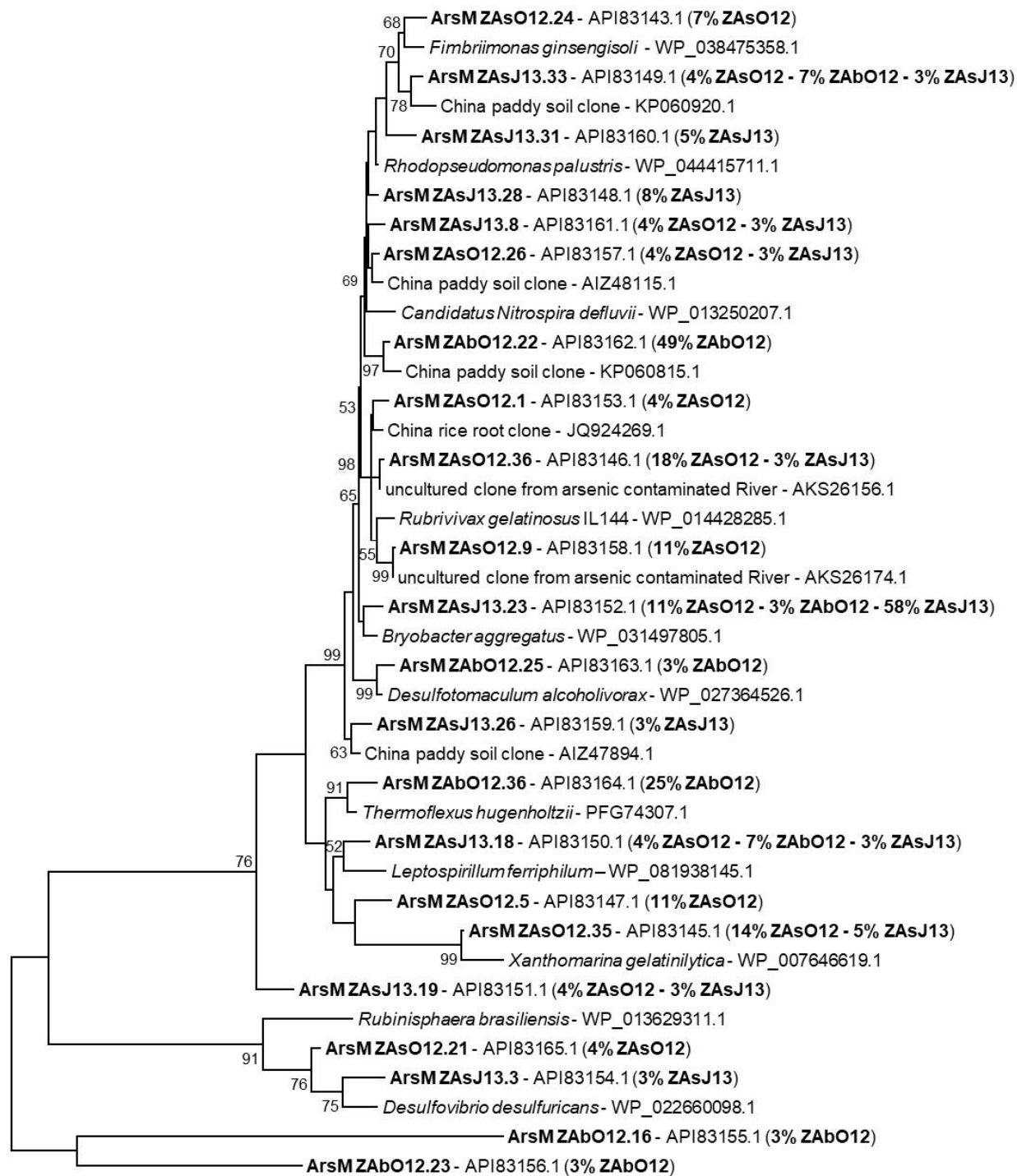
724 **Figure S2:** Rarefaction curves of *aioA* gene for the ZL1 libraries. The total number of  
725 sequences analyzed is plotted against the number of OTUs observed in the same library.

726

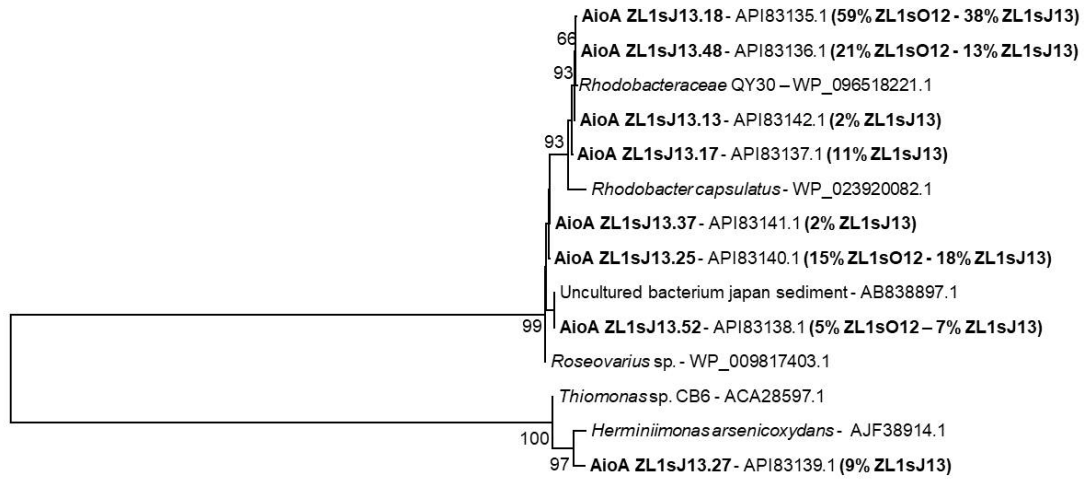
**Table 1** - Main physico-chemical parameters (temperature, pH, conductivity, redox potential, dissolved oxygen concentration), concentration of Total Organic Carbon (TOC), chlorophyll a (Chla), major anions and cations and arsenic species at the surface and at the bottom of lakes ZA and ZL1 in October 2012 and July 2013. n.d. = not determined; <DL = below detection limit

	Parameter	Unit	ZA lake				ZL1 Lake			
			October-2012		July-2013		October-2012		July-2013	
			surface	bottom (5 m)	surface	bottom (5 m)	surface	bottom (12.5 m)	surface	bottom (12.5 m)
Physico-chemical parameters	T	°C	21.8	19.8	25.7	21.8	21.5	21.1	22.3	21
	pH		8.8	8.7	8.9	8.5	9.0	9.0	9.1	9.1
	Cond.	μS/cm	7020	6930	6150	6100	15470	15490	14530	14460
	Eh	mV	361	61	399	153	312	331	336	320
	DO	mg/L	8.7	4.1	11.5	4.8	8.2	8.3	7.9	9.2
Chlorophyll	Chla	μg/L	n.d.	n.d.	7.0	n.d.	n.d.	n.d.	<1	n.d.
Total organic carbon	TOC	mg/L	39.7	40.6	30.7	28.0	4.3	5.0	2.3	2.8
Major anions and cations	CO <sub>3</sub> <sup>2-</sup>	mg/L	38	65	96	67	568	522	612	600
	HCO <sub>3</sub> <sup>-</sup>	mg/L	719	638	472	590	2147	2287	1873	1829
	Cl <sup>-</sup>	mg/L	1122	1125	1038	1022	3278	3347	3114	3046
	NO <sub>3</sub> <sup>-</sup>	mg/L	n.d.	n.d.	n.d.	n.d.	n.d.	35	n.d.	n.d.
	SO <sub>4</sub> <sup>--</sup>	mg/L	1543	1541	1466	1434	1721	1763	1742	1702
	Ca <sup>++</sup>	mg/L	50	45	38	49	n.d.	n.d.	n.d.	n.d.
	Mg <sup>++</sup>	mg/L	161	162	194	191	168	192	266	266
	Na <sup>+</sup>	mg/L	1317	1322	1321	1275	3970	4166	4085	4009
	K <sup>+</sup>	mg/L	34	38	41	35	133	115	104	103
Arsenic species	As(III)	μg/L	2.5	1.1	<DL	<DL	<DL	<DL	<DL	<DL
	DMA	μg/L	34.8	<DL	21	23	<DL	<DL	<DL	<DL
	As(V)	μg/L	<DL	<DL	14	19	115	114	142	147



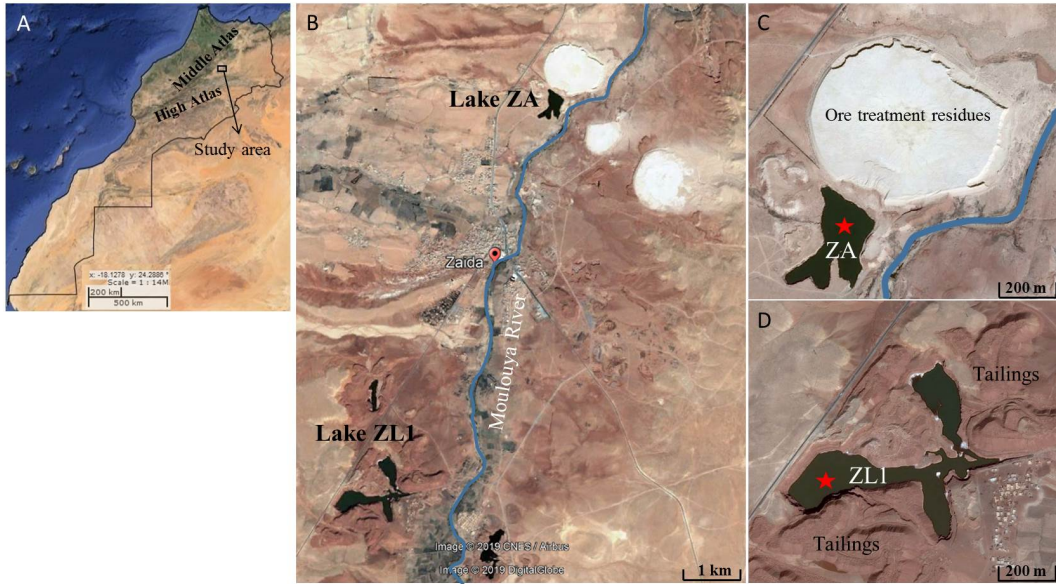


0.5



1

Journal Pre-proof



Journal Pre-proof